NASA TECHNICAL NOTE

NASA TN D-7743

NASA TN D-7743

EXPERIMENTAL INVESTIGATION OF THE BRAKING AND CORNERING CHARACTERISTICS OF 30 × 11.5-14.5, TYPE VIII, AIRCRAFT TIRES WITH DIFFERENT TREAD PATTERNS

by Robert C. Dreher and John A. Tanner

Langley Research Center
Hampton, Va. 23665

NATIONAL AERONAUTICS AND SPACE ADMINISTRATION • WASHINGTON, D. C. • OCTOBER 1974

1. Report No.	2. Government Accession No.	3. Recipient's Catalog No.
NASA TN D-7743		

4. Title and Subtitle	5. Report Date
EXPERIMENTAL INVESTIGATION OF THE BRAKING AND CORNERING CHARACTERISTICS OF 30 × 11.5-14.5, TYPE VIII, AIRCRAFT TIRES WITH DIFFERENT TREAD PATTERNS	October 1974
	6. Performing Organization Code
7. Author(s)	8. Performing Organization Report No.
Robert C. Dreher and John A. Tanner	L-9687
	10. Work Unit No.
9 Performing Organization Name and Address	501-38-12-02
NASA Langley Research Center Hampton, Va. 23665	11. Contract or Grant No.
	13. Type of Report and Period Covered
12. Sponsoring Agency Name and Address	Technical Note
National Aeronautics and Space Administration Washington, D.C. 20546	14. Sponsoring Agency Code

15. Supplementary Notes

16. Abstract

An investigation was conducted at the Langley aircraft landing loads and traction facility to study the braking and cornering characteristics of 30 × 11.5-14.5, Type VIII, aircraft tires with five different tread patterns. These characteristics, which included the drag-force and cornering-force friction coefficients, were obtained on dry, damp, and flooded runway surfaces over a range of yaw angles from 0° to 12° at ground speeds from 5 to 100 knots.

The results of this investigation indicate that a tread pattern consisting of transverse cuts across the entire width of the tread slightly improved the tire traction performance on wet surfaces. The braking and cornering capability of the tires was degraded by thin-film lubrication and tire hydroplaning effects on the wet runway surfaces. Also, the braking capability of the tires decreased when the yaw angle was increased.

17. Key Words (Suggested by Author(s))	18. Distribution Statement
Tires Aircraft Friction	Unclassified – Unlimited STAR Category 02

19. Security Classif. (of this report)	20. Security Classif. (of this page)	21. No. of Pages	22. Price*
Unclassified	Unclassified	22	$3.00

*For sale by the National Technical Information Service, Springfield, Virginia 22151

EXPERIMENTAL INVESTIGATION OF THE BRAKING AND CORNERING CHARACTERISTICS OF 30 × 11.5-14.5, TYPE VIII, AIRCRAFT TIRES WITH DIFFERENT TREAD PATTERNS

By Robert C. Dreher and John A. Tanner
Langley Research Center

SUMMARY

An investigation was conducted at the Langley aircraft landing loads and traction facility to study the braking and cornering characteristics of 30 × 11.5-14.5, Type VIII, aircraft tires with five different tread patterns. These characteristics, which included the drag-force and cornering-force friction coefficients, were obtained on dry, damp, and flooded runway surfaces over a range of yaw angles from 0° to 12° at ground speeds from 5 to 100 knots.

The results of this investigation indicate that a tread pattern consisting of transverse cuts across the entire width of the tread slightly improved the tire traction performance on wet surfaces. The braking and cornering capability of the tires was degraded by thin-film lubrication and tire hydroplaning effects on the wet runway surfaces. Also, the braking capability of the tires decreased when the yaw angle was increased.

INTRODUCTION

Researchers seek continually to improve the traction of aircraft tires on runways under adverse weather conditions. After considerable research (refs. 1 to 6, for example), they have shown that aircraft braking and steering capability decreases during wet runway operations and that the problem becomes more severe with increased ground speed and fluid depth. At higher aircraft ground speeds and at a fluid depth defined by the runway surface texture and tire tread design, the phenomenon of dynamic hydroplaning occurs wherein the tire loses contact with the runway surface and thus its directional stability and braking effectiveness. Most jet aircraft are susceptible to hydroplaning because of their high ground operating speeds.

Attempts have been made to eliminate or delay the deleterious effects attributed to hydroplaning by developing techniques which would prevent the buildup of water pressure in the tire-pavement interface. All these attempts tried to provide improved escape routes or drainage for the water in the tire footprint either by changing the texture of the

runway surface or by revising or modifying the tire tread pattern. Changing the runway surface texture through the installation of transverse grooves or the application of a porous asphalt overlay can provide increased tire traction under wet conditions (see refs. 6 and 7). Research on tire tread patterns (ref. 1, for example) has indicated that the level of friction developed by a tire on a contaminated surface is extremely sensitive to the tread design at least for fluid depths less than the tire tread depth. Traditionally, increasing the number of circumferential grooves in the tire tread, or adding radial or transverse grooves seems to improve the wet braking characteristics, particularly at the higher ground speeds. It should be noted, however, that other considerations, such as tread wear and tread integrity, during high-speed operation are limiting factors to any tread alteration.

This paper presents the results of an investigation conducted at the Langley aircraft landing loads and traction facility to determine the wet-runway performance characteristics of an aircraft tire having various tread patterns thought to improve traction under all weather conditions. Five 30 × 11.5-14.5, Type VIII, 24-ply-rating tires having different tread patterns were tested to define their braking and cornering characteristics. This size tire is presently employed on the main gear of a high performance jet fighter aircraft. The braking and cornering characteristics included the drag-force and cornering-force friction coefficients obtained for the tires operating on dry, damp, and flooded surfaces over a range of yaw angles from 0° to 12° at ground speeds from 5 to 100 knots (1 knot = 0.5144 meter/second).

The tires used in the tests were supplied by the U.S. Air Force (Rain Tire – Project 5549).

SYMBOLS

Values are given in both SI and U.S. Customary Units. The measurements and calculations were made in U.S. Customary Units. Factors relating the two systems are presented in reference 8.

μ_d drag-force friction coefficient, parallel to direction of motion, $\frac{\text{Drag force}}{\text{Vertical force}}$

$\mu_{d,max}$ maximum drag-force friction coefficient

$\mu_{d,o}$ unbraked rolling-resistance friction coefficient, parallel to direction of motion

$\mu_{d,skid}$ skidding drag-force friction coefficient

μ_s unbraked cornering-force friction coefficient, perpendicular to direction of motion, $\frac{\text{Side force}}{\text{Vertical force}}$

APPARATUS AND TEST PROCEDURE

Tires

The tires used in this investigation were 30 × 11.5-14.5, 24-ply-rating, type VIII, aircraft tires – the same type as ones employed on a current high performance jet fighter aircraft. A photograph of the test tires is presented in figure 1 which shows tire B mounted on a wheel and inflated and the remaining tires unmounted. Tire A had the standard three-groove tread configuration currently in the U.S. Air Force inventory. Tire B also had a three-groove tread pattern, but the lands were equipped with a large number of "pin" holes. For tire C, the basic tread of tire A was modified with narrow transverse cuts which connected the grooves and extended to the tire shoulders. Tire D had a four-groove tread pattern with transverse grooves in the shoulder area, and tire E was similar to tire D except for an additional circumferential groove in each shoulder. The dimensions of the various tread grooves and special features are listed in table I. All tires were tested at an inflation pressure of 1827 kPa (265 psi), and the vertical load was varied with ground speed to simulate the effects of wing lift. The loading was determined from aircraft tests and varied from approximately 73.4 kN (16 500 lb) at 5 knots to 55.6 kN (12 500 lb) at 100 knots as shown in figure 2.

Runway Surface Conditions

A concrete test runway, which was approximately 174 m (570 ft) in length, was divided into three sections so that tire braking and cornering data could be obtained on dry, damp, and flooded surfaces. The first section was kept dry to provide for full wheel spinup. The next section, 61 m (200 ft) long, was dampened (no visible standing water). The final 61 m (200 ft) section was surrounded by a dam and flooded with water to a depth of approximately 0.64 cm (0.25 in). The concrete test surface had a light broom finish which was somewhat smoother than that of most operational concrete runways. By using the grease sampling technique described in reference 3, the average texture depth of the surface in the flooded test section was measured to be 168 μm (0.0066 in.) and that in the damp section, 135 μm (0.0053 in.). A typical operational runway has an average texture depth of the order of 201 μm (0.0079 in.).

Test Facility

The investigation was performed at the Langley aircraft landing loads and traction facility, which is described in reference 9, and utilized the main test carriage pictured in figure 3. Presented in figure 4 is a schematic of the instrumented dynamometer which supported the wheel and measured the various axle loadings. The instrumentation consisted of load beams to measure vertical, drag, and side forces and links to measure brake torque. All these measurements were taken at the axle. Additional instrumentation

was provided to measure brake pressure, wheel angular velocity, and carriage displacement. Vertical, drag, and side accelerometers provided data for inertial corrections. Continuous time histories of the output of the instrumentation were recorded by an oscillograph mounted on the test carriage.

Test Procedure

The test procedure consisted of propelling or towing the test carriage across the runway test section at the desired ground speed, releasing the drop test fixture to apply the preselected vertical load on the tire, subjecting the tire to controlled brake cycles on the damp and flooded test sections, and monitoring the onboard instrumentation. In a test series the tire yaw angle was varied from 0° to 12° in 4° increments; however, it was held constant for each test run. Ground speeds for these tests ranged from 5 to 100 knots. To obtain a speed of 5 knots, the test carriage was towed by a ground vehicle; for higher speeds, the carriage was propelled by the hydraulic jet as described in reference 9. The brake cycle consisted of energizing the braking circuit with "braking cams" placed strategically along the test track, braking the tire from a free-rolling condition to a locked wheel skid, and then releasing the brake to allow tire spin-up. Time histories of the output of the instrumentation were recorded as the tire was braked on the damp and flooded test sections. In addition to the wet tests, one unyawed brake cycle was made with each tire on the dry section at a nominal ground speed of 100 knots.

RESULTS AND DISCUSSION

Tire-to-ground forces in the vertical, drag, and side directions and wheel angular velocity were recorded on an oscillograph throughout each test. These data were used to compute time histories of the drag-force friction coefficient, parallel to the direction of motion, μ_d and the unbraked cornering-force friction coefficient, perpendicular to the direction of motion, μ_s.

For each test condition, the unbraked (maximum) cornering-force friction coefficient μ_s measured just before braking was initiated, the maximum drag-force friction coefficient $\mu_{d,max}$ encountered during wheel spin-down, and the skidding drag-force friction coefficient $\mu_{d,skid}$ measured at the instant of wheel lockup were determined from faired curves representing the time history data. These data for the five test tires are presented in table II. Also included in the table are the tire unbraked rolling-resistance friction coefficient $\mu_{d,o}$. The following sections discuss the variation of $\mu_{d,max}$, $\mu_{d,skid}$, and μ_s for the five test tires with respect to both ground speed and yaw angle.

Effect of Ground Speed

The effect of ground speed on the braking and cornering characteristics for each of the five test tires is shown in figure 5 for various yaw angles and surface wetness conditions.

Maximum drag-force friction coefficient.- The maximum drag-force friction coefficients $\mu_{d,max}$ for all test tires are faired by a single curve in figure 5 for damp and flooded test conditions. In general, these fairings describe the coefficients for all tires and thus the effect of tread design seems to be insignificant. However, the data indicate that tire C provides the best traction, although, in general, the improvement is not substantial. The slightly improved performance of this tire over the others tested in this investigation may be attributed to the transverse cuts which extend across the entire width of the tread. These cuts may aid in breaking up the thin film of water on damp runway surfaces and also may help in removing bulk water from the center of the footprint on the flooded runway surfaces. Tires D and E also have transverse grooves, but only in the shoulder area; therefore, the lateral drainage in the center of the footprint is negligible.

The data presented in figure 5 show that the maximum drag-force friction coefficient $\mu_{d,max}$ decreases with increasing ground speed on both the damp and flooded test surfaces. This trend, which can be attributed to thin-film lubrication and hydroplaning effects, is noted for all test yaw angles. Values of $\mu_{d,max}$ at 0° yaw range from about 0.6 at 5 knots, which is in good agreement with that predicted (0.64) from the empirical expression developed in reference 10 at very low ground speeds, to approximately 0.2 at 100 knots. Generally lower values of $\mu_{d,max}$ are associated with the introduction of yaw at all speeds. The values of $\mu_{d,max}$ at lower speeds are typically greater on the flooded surface than those obtained on the damp surface probably because of the higher average texture depth of the surface in the flooded test section. At high speeds, the effect of dynamic hydroplaning is more pronounced, particularly on the flooded surface, and $\mu_{d,max}$ is generally higher on the damp surface than on the flooded surface. Note, however, that $\mu_{d,o}$ listed in table II is greater in the flooded section at high speeds because of fluid drag.

The values of $\mu_{d,max}$ obtained on a dry surface for the five test tires unyawed at a ground speed of 100 knots are shown in figure 5(a) by the closed symbols. These data show very little difference among the tires.

Skidding drag-force friction coefficient.- The ground speed also affects the skidding drag-force friction coefficient $\mu_{d,skid}$. The data presented in figure 5 show that on both

the damp and flooded surfaces, the values of $\mu_{d,skid}$ decrease rapidly as the ground speed is increased from 5 knots to 50 knots with a less pronounced decrease for further increases in ground speed. Tire C generally displays a slightly higher $\mu_{d,skid}$ than the other tires for possibly the same reasons discussed in the previous section. As noted in table II, $\mu_{d,skid}$ and $\mu_{d,max}$ values are identical at 5 knots as expected (ref. 1), but interestingly at 100 knots the value of $\mu_{d,skid}$ for each tire except tire D is approximately 0.10 on all surfaces at all test yaw angles.

Unbraked cornering-force friction coefficient.- As observed from the time histories of the recorded data, the cornering-force friction coefficient μ_s obtained from the test tires under yawed rolling conditions decreased with brake application to a negligible value at wheel lockup. Thus, the maximum value of μ_s occurred during free rolling conditions and, as shown in figure 5, decreases in magnitude as the ground speed increases. Very little difference can be noted in μ_s among the tires, although tire C appears to have slightly better cornering capability under some conditions, particularly at the higher yaw angles.

Effect of Yaw Angle

The significant data from table II are presented in figure 6 to show more clearly the effect of yaw angle on the maximum and skidding values of the drag-force friction coefficient and the unbraked (maximum) cornering-force friction coefficient obtained from the different tire tread designs at various ground speeds and surface wetness conditions.

Maximum drag-force friction coefficient.- The data presented in figure 6 indicate that the highest values of $\mu_{d,max}$ occur for the unyawed tire and generally decrease with increasing yaw angle. Such a trend is more pronounced at a ground speed of 5 knots. Figure 6, however, better illustrates that at the lower ground speeds the $\mu_{d,max}$ obtained on the flooded runway is generally higher than that obtained on the damp runway; as noted previously, this result is attributed to the rougher surface texture in the flooded runway test section.

Skidding drag-force friction coefficient.- As pointed out earlier, the skidding and maximum drag-force friction coefficients at 5 knots are the same for each tire and surface condition; thus, comments relative to $\mu_{d,max}$ at that speed are appropriate to $\mu_{d,skid}$. For ground speeds of 50 and 100 knots, $\mu_{d,skid}$ is essentially independent of yaw angle and the surface wetness condition. Only at 5 knots are surface texture effects observable; that is, $\mu_{d,skid}$ values are higher on the flooded runway than on the damp runway.

Unbraked cornering-force friction coefficient.- The maximum or unbraked cornering-force friction coefficient is shown in figure 6 to vary with yaw angle in an expected manner (refs. 11 and 12). At 5 knots, μ_s increases with increasing yaw angle

up to and including the maximum test angle on both the damp and flooded surfaces. At the higher test speeds, μ_s peaks within the range of test yaw angles: between 4° and 8° at 50 knots and at approximately 4° at 100 knots.

SUMMARY OF RESULTS

Tests were conducted at the Langley aircraft landing loads and traction facility to determine the braking and cornering characteristics of $30 \times 11.5\text{-}14.5$, type VIII, aircraft tires having five different tread patterns. These characteristics, which included the drag-force and cornering-force friction coefficients, were obtained on dry, damp, and flooded runway surfaces over a range of yaw angles from 0° to 12° and at ground speeds from 5 to 100 knots. The results from the tests are summarized as follows:

1. The drag-force and cornering-force friction coefficients for the transversely grooved tire C were shown to be slightly higher than those of the other tires in this investigation.

2. The maximum drag-force friction coefficient was shown to (a) decrease with increased ground speed for all test conditions, (b) decrease as the yaw angle was increased from 0° to 12°, and (c) be higher on the flooded runway with greater texture depth than on the damp runway with less texture depth at low ground speeds.

3. The skidding drag-force friction coefficient was shown to (a) decrease with increased ground speed for all test conditions, (b) decrease as the yaw angle was increased from 0° to 12° at 5 knots, and (c) be essentially independent of yaw angle at 50 and 100 knots.

4. The unbraked cornering-force friction coefficient for all tires was shown to (a) decrease with increased ground speed for constant yaw angles above 0°, (b) increase as the yaw angle is increased from 0° to 12° at 5 knots, (c) reach peak values between 4° and 8° at 50 knots, and (d) reach peak values at approximately 4° at 100 knots.

The results of this investigation indicate that changes in the tire tread pattern from the standard tread configurations provide, at best, marginal improvements in tire braking and cornering performance on wet runways. These results in turn would suggest that runway surface treatments, such as pavement grooving and porous overlays, may be the more efficient way of improving aircraft ground performance during wet runway operations.

Langley Research Center,
National Aeronautics and Space Administration,
Hampton, Va., August 22, 1974.

REFERENCES

1. Horne, Walter B.; and Leland, Trafford, J. W.: Influence of Tire Tread Pattern and Runway Surface Condition on Braking Friction and Rolling Resistance of a Modern Aircraft Tire. NASA TN D-1376, 1962.

2. Horne, Walter B.; and Dreher, Robert C.: Phenomena of Pneumatic Tire Hydroplaning. NASA TN D-2056, 1963.

3. Leland, Trafford J. W.; Yager, Thomas J.; and Joyner, Upshur T.: Effects of Pavement Texture on Wet-Runway Braking Performance. NASA TN D-4323, 1968.

4. Horne, Walter B.; Yager, Thomas J.; and Taylor, Glenn R.: Review of Causes and Alleviation of Low Tire Traction on Wet Runways. NASA TN D-4406, 1968.

5. Byrdsong, Thomas A.: Investigation of the Effect of Wheel Braking on Side-Force Capability of a Pneumatic Tire. NASA TN D-4602, 1968.

6. Yager, Thomas J.; Phillips, W. Pelham; Horne, Walter B.; and Sparks, Howard C. (With appendix D by R. W. Sugg): A Comparison of Aircraft and Ground Vehicle Stopping Performance on Dry, Wet, Flooded, Slush-, Snow-, and Ice-Covered Runways. NASA TN D-6098, 1970.

7. Anon.: Pavement Grooving and Traction Studies. NASA SP-5073, 1968.

8. Anon.: Metric Practice Guide. E 380-72, Amer. Soc. Testing & Mater., June 1972.

9. Tanner, John A.: Fore-and-Aft Elastic Response Characteristics of 34 × 9.9, Type VII, 14 Ply-Rating Aircraft Tires of Bias-Ply, Bias-Belted, and Radial-Belted Design. NASA TN D-7449, 1974.

10. Smiley, Robert F.; and Horne, Walter B.: Mechanical Properties of Pneumatic Tires With Special Reference to Modern Aircraft Tires. NASA TR R-64, 1960. (Supersedes NACA TN 4110.)

11. Dreher, Robert C.; and Tanner, John A.: Experimental Investigation of the Cornering Characteristics of a C40 × 14-21 Cantilever Aircraft Tire. NASA TN D-7203, 1973.

12. Tanner, John A.; and Dreher, Robert C.: Cornering Characteristics of a 40 × 14-16 Type VII Aircraft Tire and and Comparison With Characteristics of a C40 × 14-21 Cantilever Aircraft Tire. NASA TN D-7351, 1973.

TABLE I.- TIRE TREAD GROOVE DIMENSIONS

Tire	Number of circumferential grooves	Groove dimensions, Width × Depth, cm (in.)	Special features	Feature dimensions, Width × Depth, cm (in.)
A	3	1.27 × 0.79 (1/2 × 5/16)	None	----------
B	3	0.64 × 0.56 (1/4 × 7/32)	Pinholes	0.16 diam × 0.64 deep (1/16 diam × 1/4 deep)
C	3	1.27 × 0.79 (1/2 × 5/16)	Transverse cuts across tread	Alternating 0.12 × 0.64, 0.16 × 0.48 (3/64 × 1/4, 1/16 × 3/16)
D	4	0.95 × 0.64 (3/8 × 1/4)	Transverse grooves shoulder only	0.79 × 0.64 (5/16 × 1/4)
E	6	0.95 × 0.64 (3/8 × 1/4)	Transverse grooves shoulder only	0.79 × 0.64 (5/16 × 1/4)

TABLE II.- SUMMARY OF FRICTION COEFFICIENTS OBTAINED FOR VARIOUS TEST CONDITIONS

Tire	Yaw angle, deg	Vertical load		Ground speed, knots	Dry or damp surface				Flooded surface			
		kN	lbf		$\mu_{d,max}$	$\mu_{d,skid}$	μ_s	$\mu_{d,o}$	$\mu_{d,max}$	$\mu_{d,skid}$	μ_s	$\mu_{d,o}$
A	0	68.5	15 397	105	*0.6	*0.1	*0	*0.03	---	---	---	---
	0	76.3	17 160	5	.56	.56	0	.02	0.63	0.63	0	0.02
	0	70.9	15 944	33	.38	.22	0	.03	.42	.26	0	.04
	0	67.0	15 055	47	.35	.20	0	.03	.40	.22	0	.04
	0	58.9	13 250	75	.30	.14	0	.03	.28	.16	0	.07
	0	52.5	11 811	98	.30	.16	0	.01	.22	.14	0	.09
	4	75.4	16 963	5	.46	.46	.27	.04	.43	.43	.30	.04
	4	67.1	15 077	46	.32	.20	.19	.04	.32	.20	.22	.04
	4	52.7	11 840	100	.17	.09	.14	.035	.13	.06	.09	.06
	8	76.2	17 139	5	.36	.36	.31	.06	.40	.40	.34	.04
	8	67.6	15 200	46	.24	.19	.20	.05	.28	.24	.21	.06
	8	53.6	12 053	101	.15	.10	.10	.06	.12	.09	.04	.09
	12	60.5	13 600	5	.36	.36	.32	.09	.42	.42	.43	.11
	12	66.8	15 016	51	.24	.23	.16	.07	.24	.20	.16	.07
	12	54.4	12 235	101	.13	.09	.10	0	.12	.12	.06	.10
B	0	57.9	13 019	101	*0.55	*0.08	*0	*0.02	---	---	---	---
	0	77.6	17 444	5	.64	.64	0	.03	0.62	0.62	0	0.04
	0	73.8	16 600	33	.40	.18	0	.03	.42	.23	0	.04
	0	65.8	14 793	56	.36	.16	0	.05	.32	.18	0	.08
	0	60.1	13 500	70	.40	.14	0	.02	.28	.22	0	.07
	0	56.3	12 660	103	.20	.13	0	.02	.2	.14	0	.08
	4	75.9	17 056	5	.38	.38	.25	.03		.47	.28	.04
	4	69.3	15 569	52	.34	.18	.22	.03		.16	.16	.04
	4	52.9	11 883	102	.24	.08	.21	.05		.10	.06	.10
	8	74.8	16 813	5	.38	.38	.32	.07	.2	.42	.39	.07
	8	50.7	11 394	53	.26	.16	.18	.06	.18	.16	.14	.06
	8	51.6	11 590	102	.19	.07	.13	.04	.08	.08	.03	.08
	12	80.5	18 103	5	.40	.40	.33	.09	.44	.44	.40	.11
	12	65.9	14 814	53	.19	.16	.18	.09	.20	.20	.13	.08
	12	51.3	11 523	103	.11	.11	.07	.05	.16	.15	0	.10
C	0	55.6	12 500	98	*0.58	*0.12	*0	*0.02	---	---	---	---
	0	74.7	16 800	5	.57	.57	0	.04	0.64	0.64	0	0.03
	0	72.1	16 200	32	.52	.27	0	.03	.42	.32	0	.03
	0	67.2	15 100	51	.44	.22	0	.04	.40	.30	0	.08
	0	63.2	14 200	74	.42	.17	0	.03	.36	.22	0	.08
	0	53.8	12 100	106	.26	.10	0	.04	.18	.13	0	.08
	4	75.2	16 900	5	.46	.46	.27	.04	.60	.60	.31	.06

*Dry surface.

TABLE II.- SUMMARY OF FRICTION COEFFICIENTS OBTAINED FOR VARIOUS TEST CONDITIONS - Concluded

Tire	Yaw angle, deg	Vertical load		Ground speed, knots	Dry or damp surface				Flooded surface			
		kN	lbf		$\mu_{d,max}$	$\mu_{d,skid}$	μ_s	$\mu_{d,o}$	$\mu_{d,max}$	$\mu_{d,skid}$	μ_s	$\mu_{d,o}$
C	4	68.9	15 500	54	0.28	0.16	0.21	0.03	0.30	0.22	0.21	0.04
	4	51.2	11 500	103	.20	.10	.20	.04	.17	.09	.06	.09
	8	80.5	18 100	5	.37	.37	.34	.07	.47	.47	.42	.08
	8	71.2	16 000	40	.28	.20	.22	.04	.36	.21	.29	.07
	8	52.5	11 80	100	.20	.14	.16	.06	.18	.15	.06	.12
	12	77.8	17 500	5	.46	.46	.41	.13	.51	.51	.49	.16
	12	67.2	15 100	50	.26	.18	.23	.09	.24	.22	.23	.09
	12	55.6	12 500	99	.12	.10	.15	.07	.16	.10	.07	.10
D	0	57.8	13 000	95	*0.56	*0.15	*0	*0.04	---	---	---	---
	0	75.6	17 000	5	.64	.64	0	.03	0.65	0.65	0	0.03
	0	77.0	17 300	30	.44	.23	0	.02	.44	.26	0	.03
	0	68.5	15 400	53	.31	.18	0	.02	.28	.18	0	.04
	0	60.9	13 700	70	.29	.18	0	.04	.30	.20	0	.06
	0	54.3	12 200	102	.21	.12	0	.06	.14	.12	0	.07
	4	77.4	17 400	5	.41	.41	.26	.03	.46	.46	.27	.03
	4	66.7	15 000	50	.24	.20	.20	.03	.20	.17	.20	.05
	4	52.9	11 900	100	.12	.10	.18	.04	.0	.10	.07	.09
	8	83.6	18 800	5	.40	.40	.32	.07	.42	.42	.36	.08
	8	68.5	15 400	54	.19	.13	.20	.04	.20	.18	.19	.06
	8	53.8	12 100	106	.11	.06	.12	.03	.12	.07	.09	.07
	12	73.4	16 500	5	.44	.44	.36	.10	.48	.48	.41	.13
	12	66.7	15 000	51	.22	.22	.20	.05	.20	.16	.20	.05
	12	53.8	12 100	103	0	0	.15	0	0	0	.07	0
E	0	52.7	11 849	100	*0.60	*0.11	*0	*0.02	---	---	---	---
	0	75.5	16 971	5	.64	.64	0	.03	0.64	0.64	0	0.03
	0	73.0	16 412	33	.39	.20	0	.02	.40	.24	0	.04
	0	65.4	14 701	54	.30	.21	0	.02	.24	.20	0	.04
	0	60.9	13 698	71	.27	.16	0	.04	.28	.20	0	.06
	0	56.3	12 652	97	.20	.08	0	.06	.17	.13	0	.09
	4	78.6	17 668	5	.40	.40	.23	.05	.54	.54	.27	.03
	4	68.4	15 383	53	.26	.22	.18	.04	.23	.14	.22	.05
	4	53.9	12 113	101	.18	.10	.14	.04	.15	.15	.08	.10
	8	81.5	18 328	5	.36	.36	.27	.05	.51	.51	.37	.08
	8	61.3	13 790	50	.28	.18	.20	.08	.23	.16	.23	.07
	8	57.8	12 989	102	.09	.08	.10	0	.11	.10	.06	.08
	12	79.1	17 790	5	.36	.36	.31	.07	.42	.42	.39	.11
	12	67.4	15 154	54	.18	.16	.16	.06	.22	.19	.18	.10
	12	57.2	12 858	101	.09	.09	.05	.08	.11	.11	.06	.08

*Dry surface.

L-73-4543.1

Figure 1.- Photograph of the five test tires showing the various tread patterns.
(Tire B mounted and inflated.)

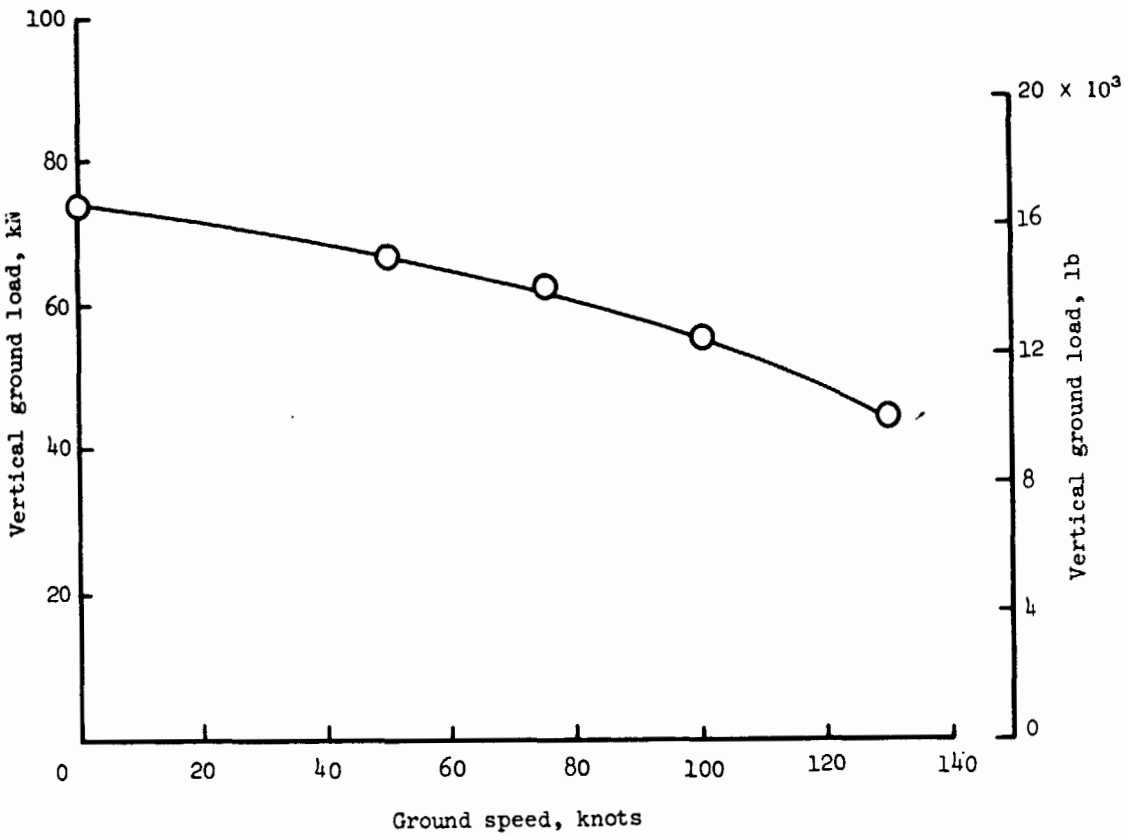

Figure 2.- Variation of tire vertical ground load with ground speed. (Unpublished data obtained from flight tests.)

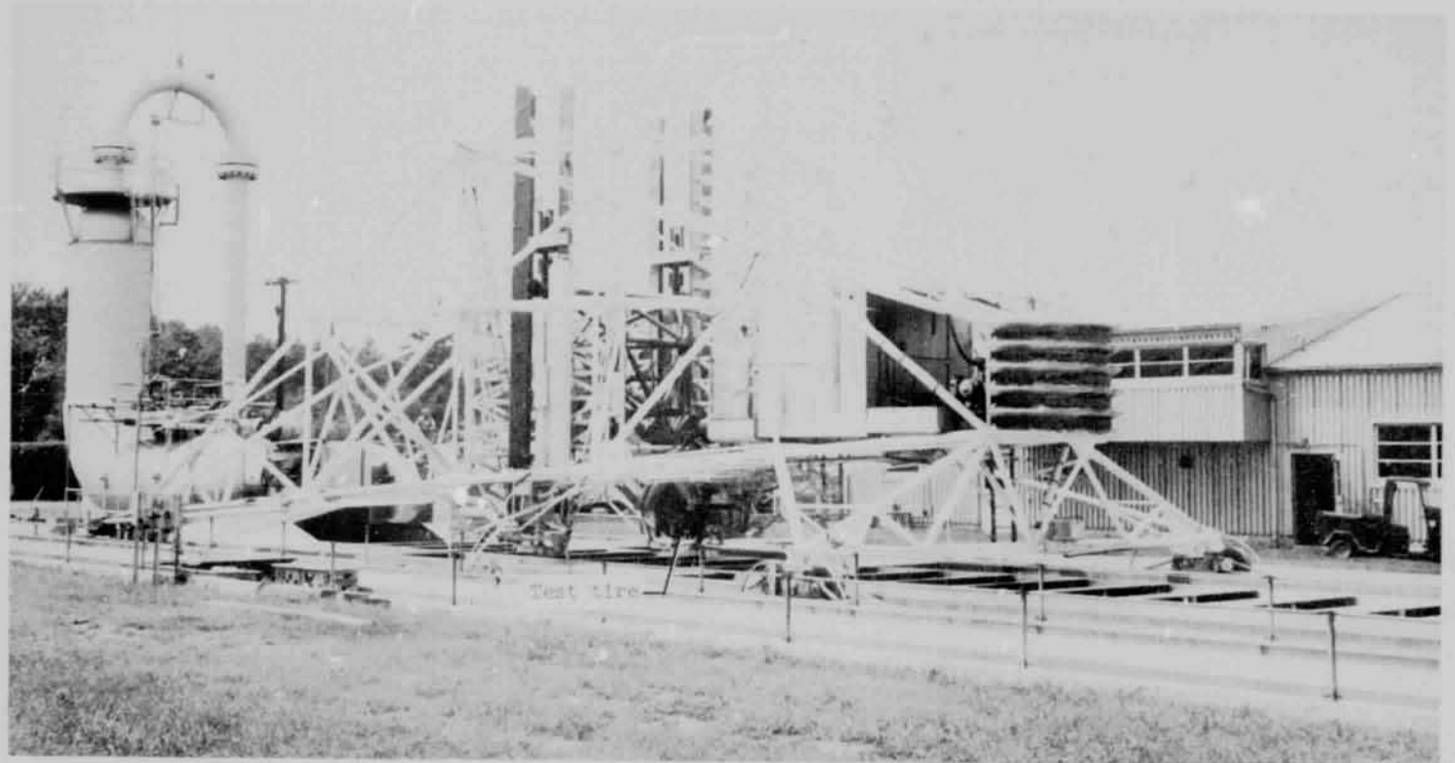

L-69-5860.1

Figure 3.- Main test carriage at Langley aircraft landing loads and traction facility.

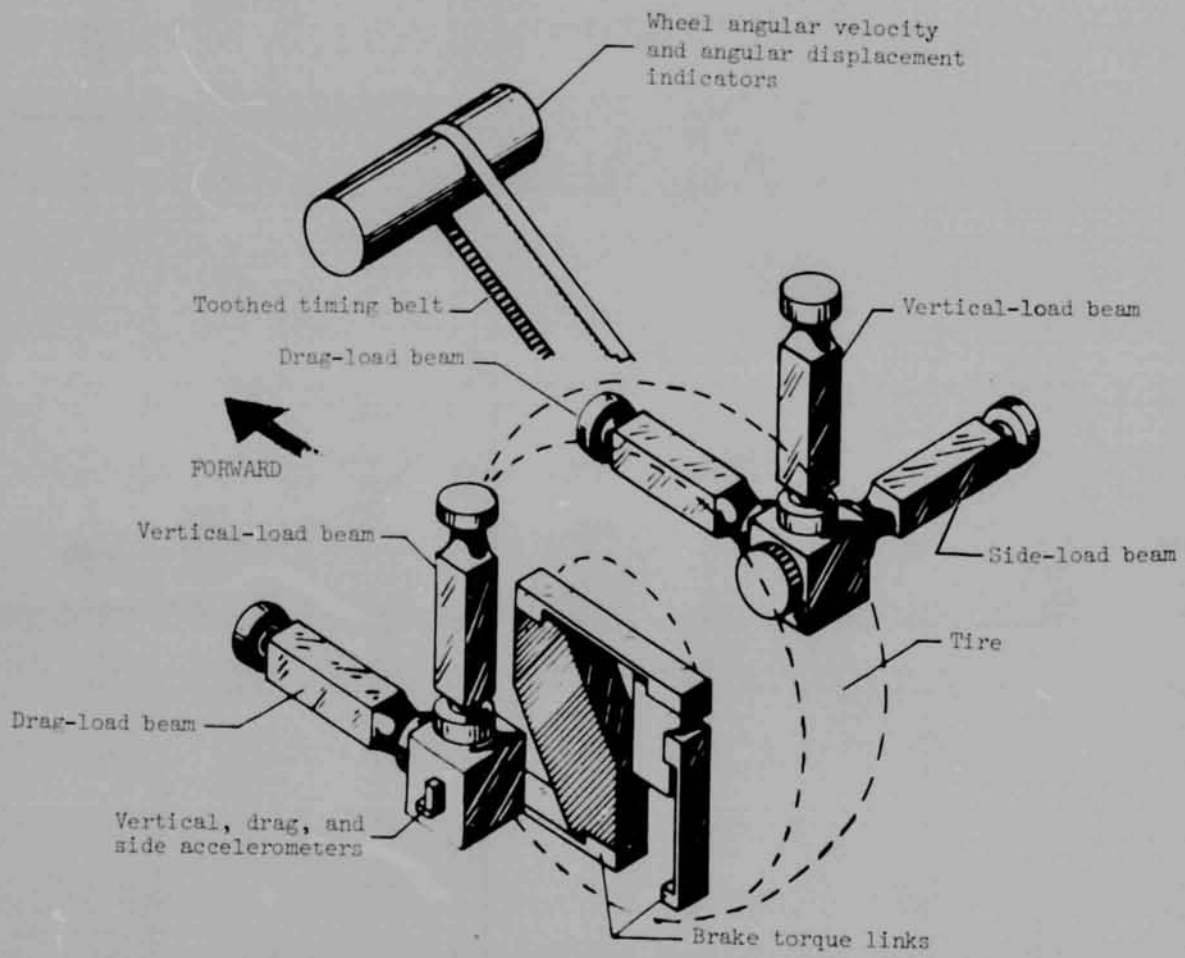

Figure 4.- Schematic of dynamometer used in tests.

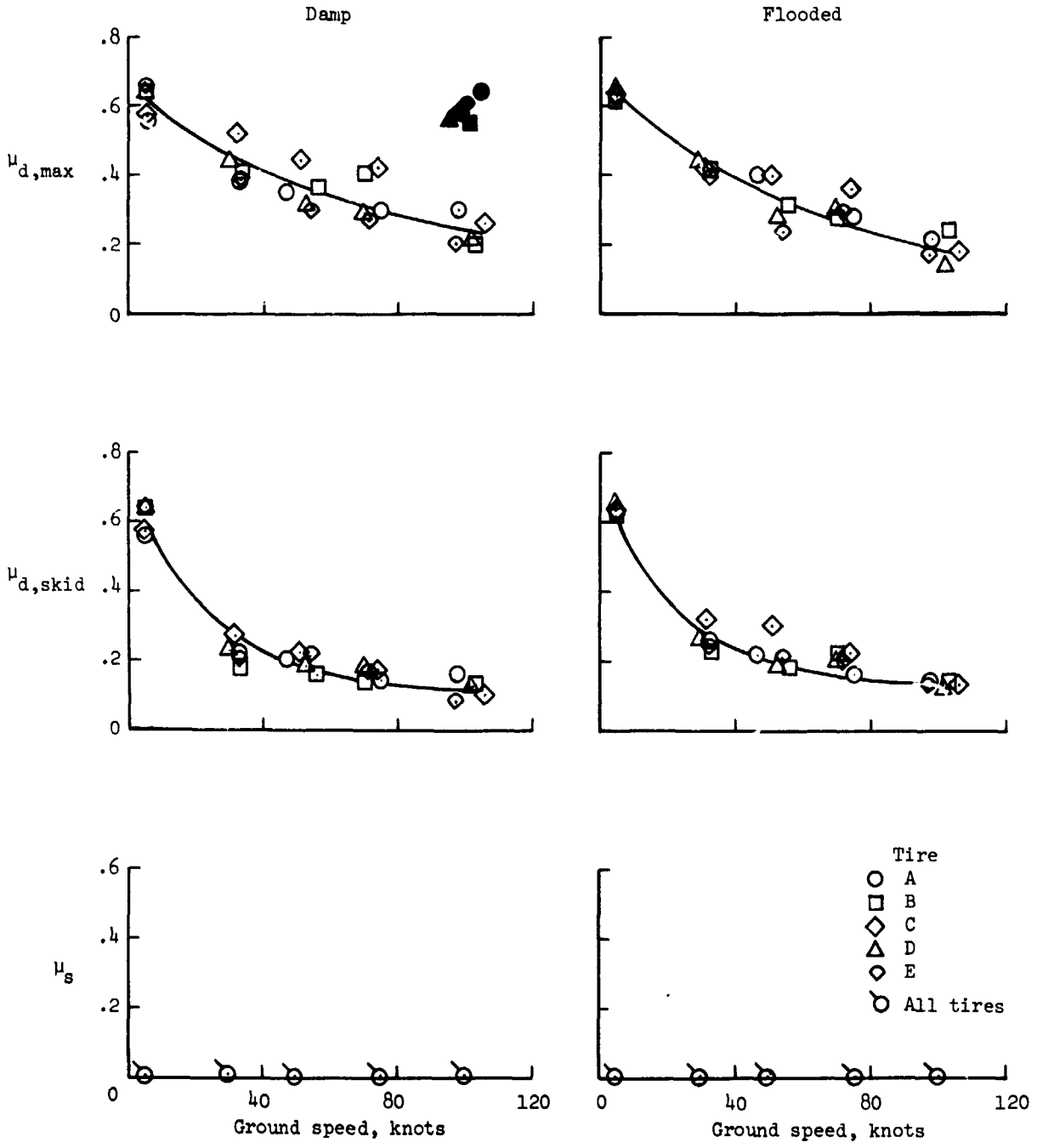

(a) Yaw angle = 0^o.

Figure 5.- Effect of ground speed on maximum drag-force friction coefficient $\mu_{d,max}$, skidding drag-force friction coefficient $\mu_{d,skid}$, and unbraked (maximum) cornering-force friction coefficient μ_s at various yaw angles for the five test tires on damp and flooded surfaces. (Closed symbols denote dry surface.)

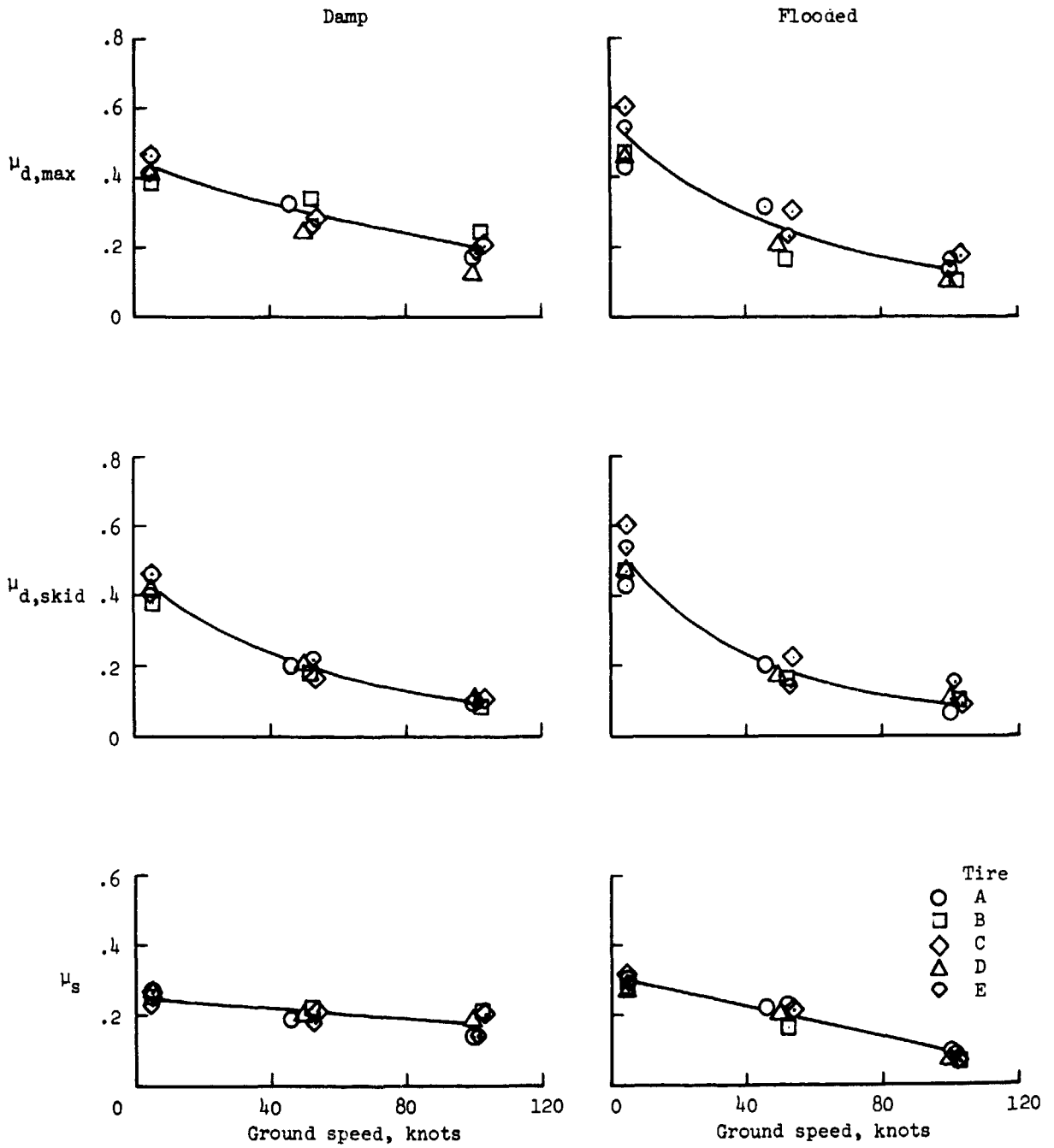

(b) Yaw angle = 4°.

Figure 5.- Continued.

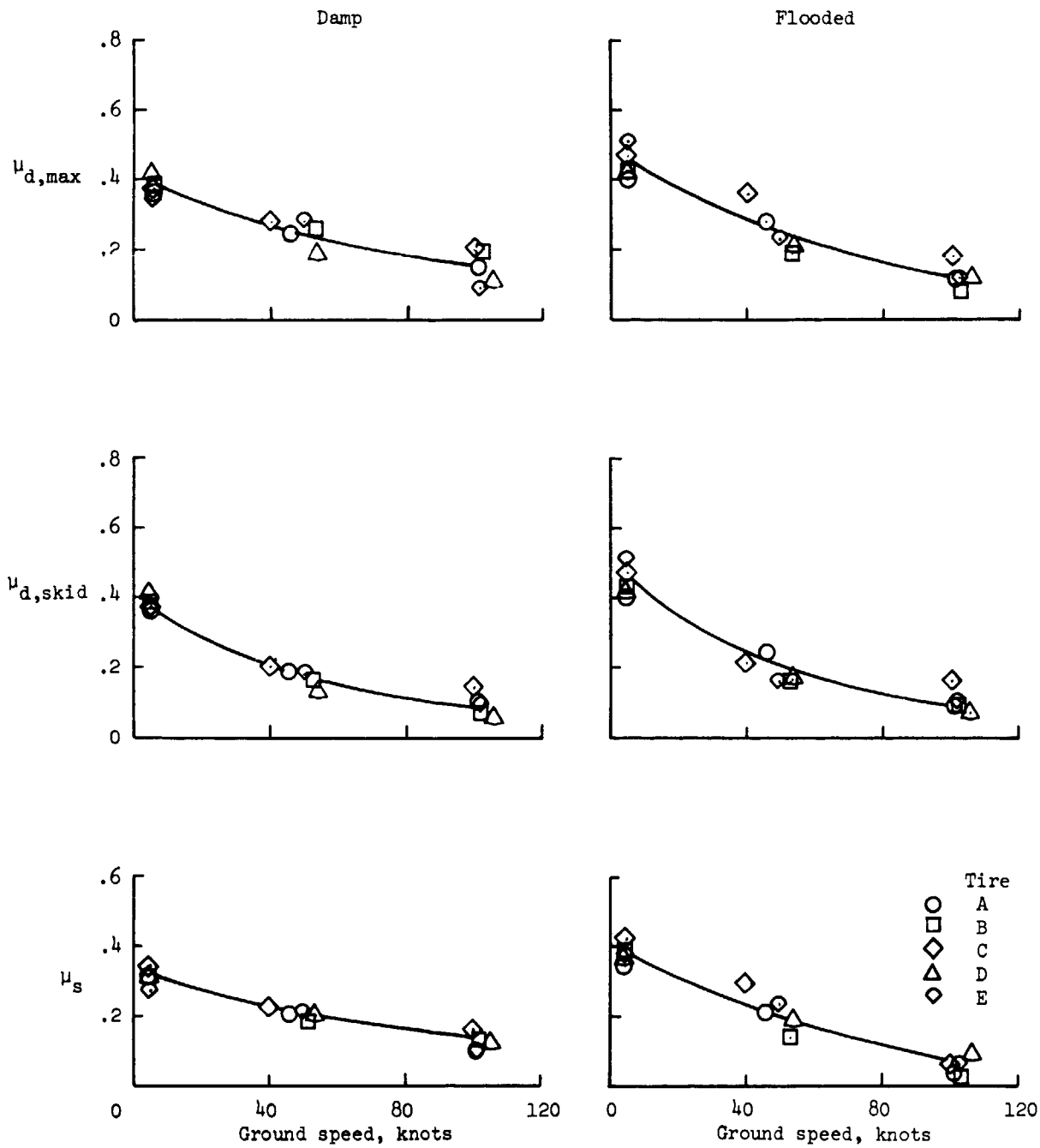

(c) Yaw angle = 8°.

Figure 5.- Continued.

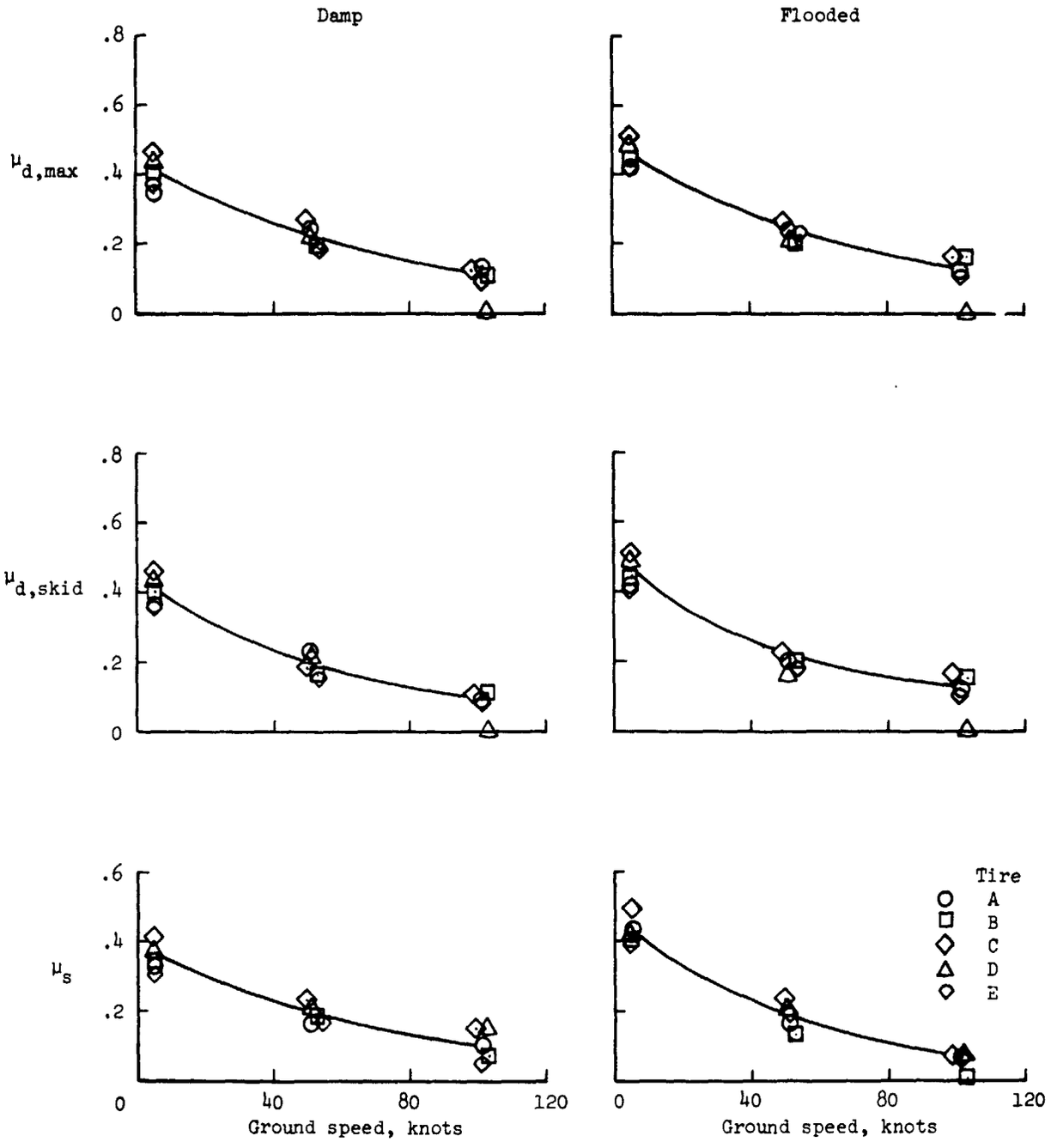

(d) Yaw angle = 12°.

Figure 5.- Concluded.

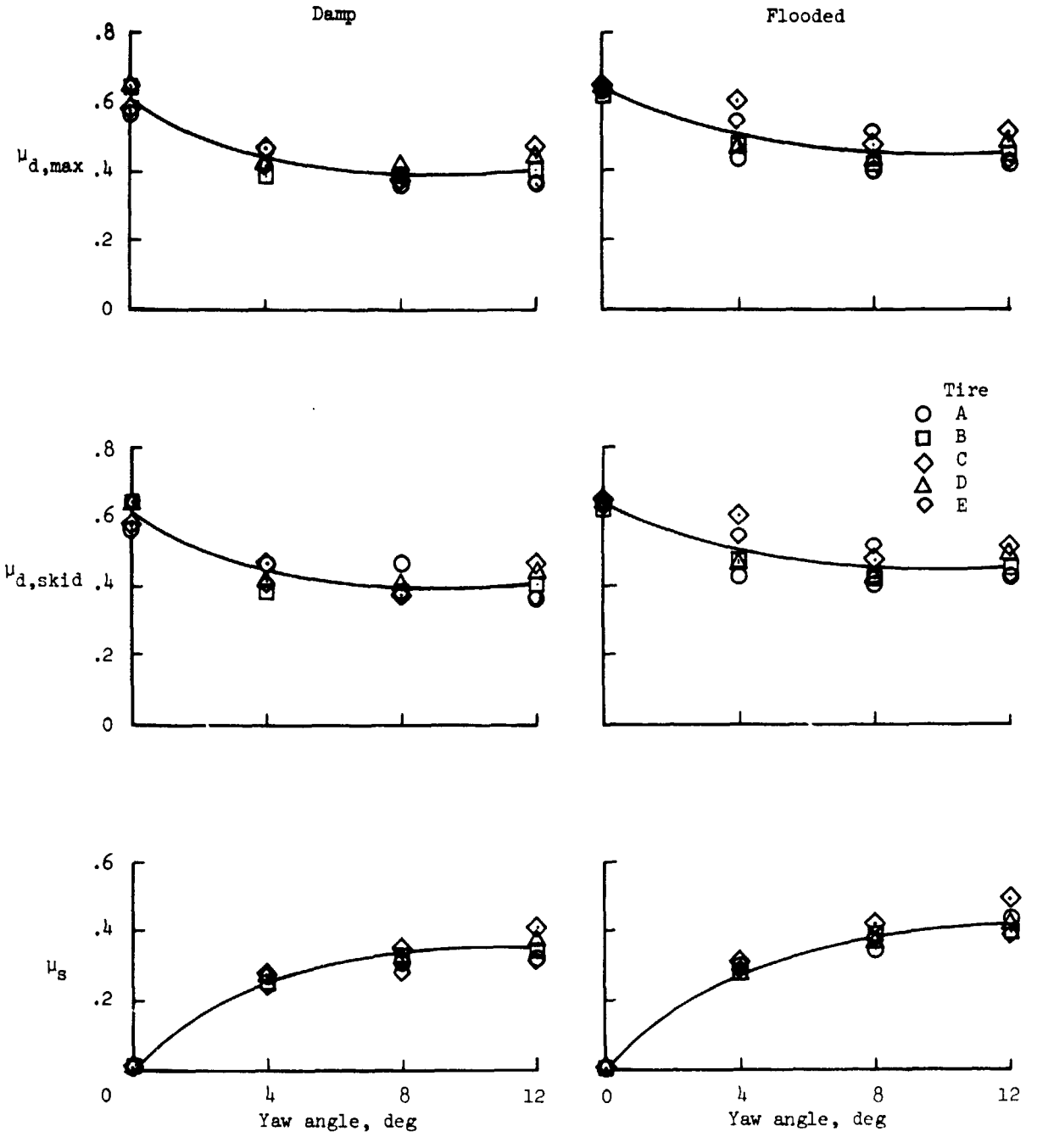

(a) Ground speed ≈ 5 knots.

Figure 6.- Effect of yaw angle on maximum drag-force friction coefficient $\mu_{d,max}$, skidding drag-force friction coefficient $\mu_{d,skid}$, and unbraked (maximum) cornering-force friction coefficient μ_s at various ground speeds for the five test tires on damp and flooded surfaces.

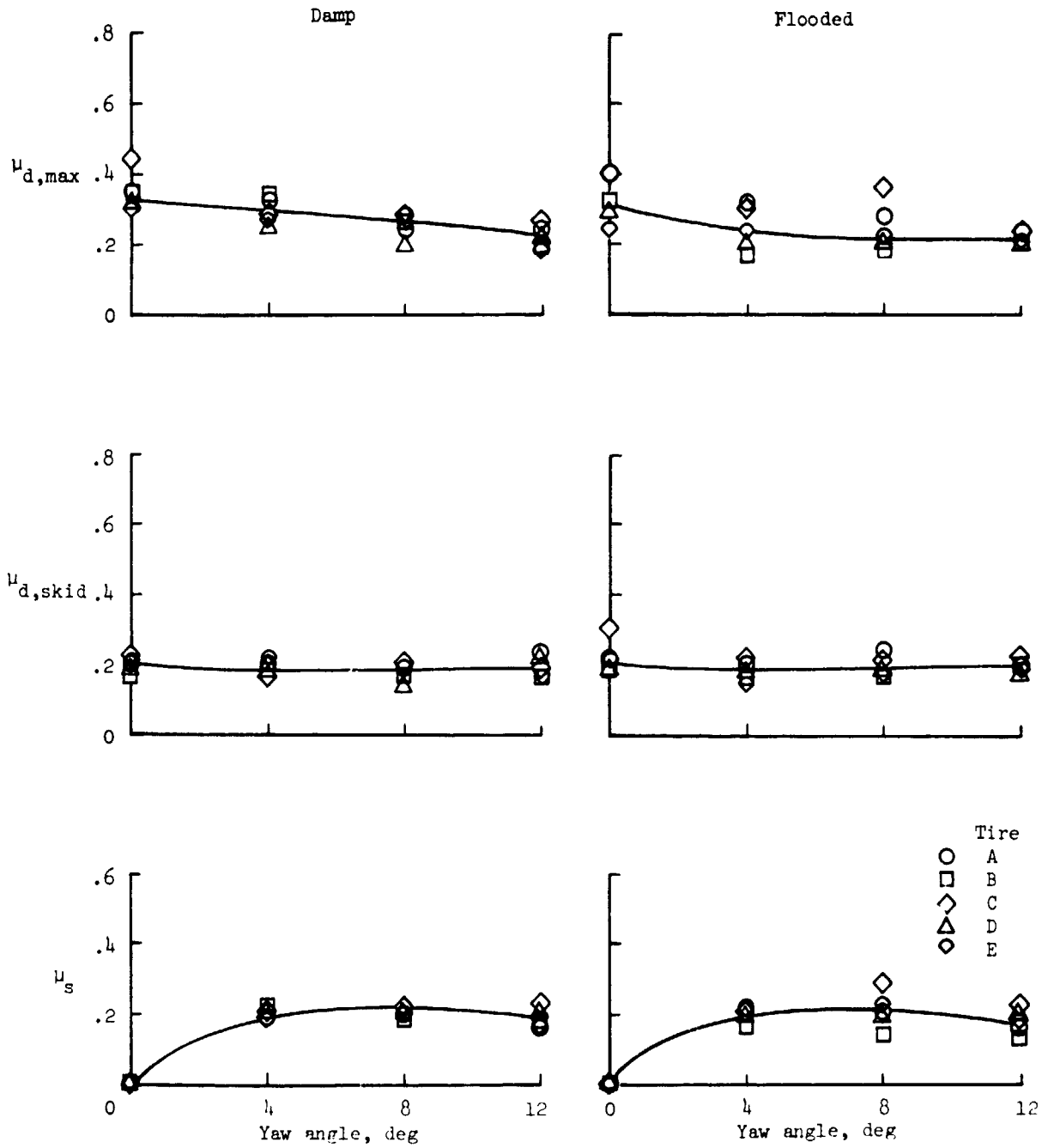

(b) Ground speed ≈ 50 knots.

Figure 6.- Continued.

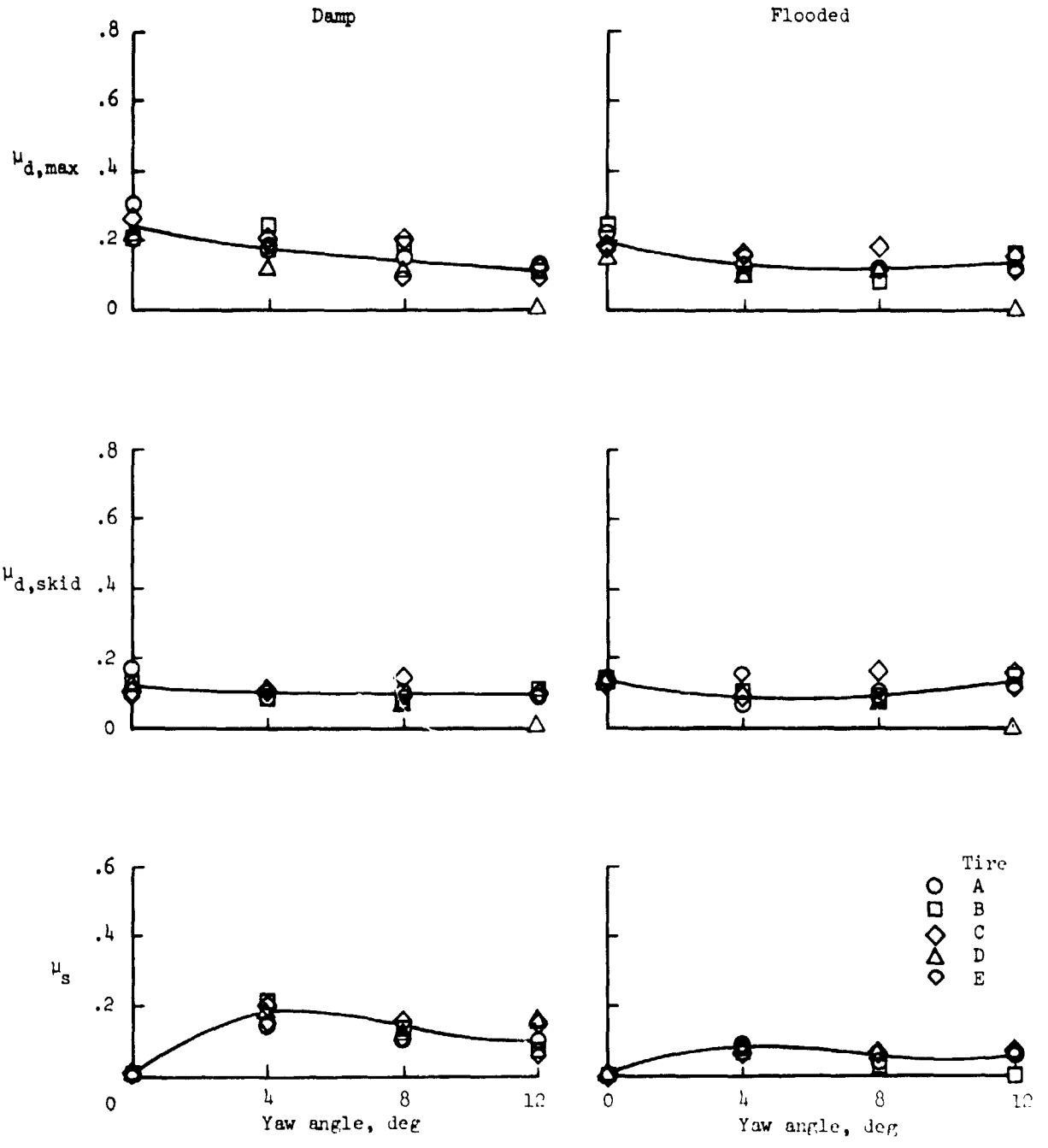

(c) Ground speed ≈ 100 knots.

Figure 6.- Concluded.